Jurnal Matematika Vol. 14, No.1, Juni 2024, pp. 11-21 ISSN: 1693-1394
Article DOI: 10.24843/JMAT.2024.v14.i01.p168

Numerical Implementation of Various Boundary Conditions on the Shallow Water Equation using a Novel Conformal and Non-conformal Finite Element Methods

Putu Veri Swastika
Department of Mathematics, Faculty of Mathematics and Natural Sciences, Udayana University, Jl. Raya Kampus UNUD, Bukit Jimbaran, Badung, Bali, Indonesia
Email: veriswastika@unud.ac.id

Rani Sulvianuri
Industrial and Financial Mathematics Research Group, Faculty of Mathematics and Natural Sciences, Institut Teknologi Bandung, Jalan Ganesha 10, Bandung 40132, Indonesia
Email: ranisulvianuri@gmail.com

I Putu Winada Gautama
Department of Mathematics, Faculty of Mathematics and Natural Sciences, Udayana University, Jl. Raya Kampus UNUD, Bukit Jimbaran, Badung, Bali, Indonesia
Email: winadagautama@unud.ac.id

Abstract**:** *In this paper, we extend the capability of a newly developed numerical scheme based on our preceding linear conformal and non-conformal finite element methods (FEM) to study 2D shallow water equations (SWE) with various boundaries. Unlike the usual approach, we approximate the unknown in a staggered grid due to the use of a linear alternating basis. Here, the free surface is approximated using a conformal while the velocity potential is approximated using a non-conformal lin-ear basis. As a result, the variational problem must be reformulated. The resulting scheme is an ODE system which is easy to solve by any time integration method. Therefore, our method is stag-gered in space, explicit, flexible and simple to implement. The simulation results show that the flexibility of the scheme can be interpreted as the successful use of various boundary conditions.*

Keywords*: 2D SWE, staggered finite element, non-conformal basis, influx boundary*

Abstrak**:** *Dalam makalah ini, kami mengembangkan lebih jauh kapabilitas skema numerik yang baru dikembangkan pada penelitian sebelumnya, berdasarkan pada metode elemen (FEM) konformal dan non-konformal linier untuk mempelajari persamaan air dangkal 2D dengan penerapan berbagai kondisi batas. Berbeda dengan pendekatan pada umumnya, kami menghitung variabel yang tidak diketahui pada grid bertingkat (staggered) akibat penggunaan basis linier secara selang seling; basis konformal dan non-konformal. Variabel permukaan bebas dihampiri menggunakan basis konformal sedangkan kecepatan potensial dihampiri dengan basis non-konformal. Akibatnya, bentuk variasional permasalahan harus diformulasikan ulang. Skema yang*

dihasilkan adalah sistem ODE yang mudah diselesaikan dengan sebarang metode integrasi waktu. Oleh karena itu, metode kami bersifat staggered in space, eksplisit, fleksibel, dan mudah diterapkan. Hasil simulasi menunjukkan bahwa sifat fleksibilitas skema dapat artikan sebagai keberhasilan penggunaan berbagai kondisi batas yang diterapkan secara bersamaan dalam skema.

***Kata Kunci**: 2D SWE, metode elemen hingga pada grid bertingkat, basis non-konformal, syarat batas fluks masuk.*

1. Introduction

One of the equations that are often used in modelling in shallow areas is the Shallow Water Equation (SWE). It consists of a system of nonlinear first-order partial differential equations, i.e. mass continuity and momentum balance. This equation is derived from the Navier Stokes equation with the shallow assumption, namely the horizontal length scale is more dominant than the depth scale, so the vertical velocity component can be neglected. Thus, the SWE equation can be used to model various phenomena in shallow areas such as: steady flow in open channels (Hadiarti et al., 2023; Swastika et al., 2021), nearshore tsunami propagation (Tarwidi et al., 2022), internal wave(Swastika & Pudjaprasetya, 2021), etc.

It is difficult to determine the exact solution of the SWE equation, especially when it is applied to mimic real-world occurrences. As a result, numerical approximation is an alternate method for obtaining the SWE solution. The finite element method is one method that several authors frequently employ to solve the SWE (Hanert et al., 2003; Le Roux et al., 2005). In general, the finite element approach is a methodology for constructing finite-dimensional spaces of a Hilbert space of specific classes of functions, such as Sobolev spaces of various orders and their subspaces, in order to apply the Galerkin process to a variational problem or weak formulation (Siddiqi, 2018).

In our preceding contribution (Swastika et al., 2020), we proposed a newly non-conformal P_1^{NC} basis function. Our work was inspired by Hua & Tommaset (1984) and Cui (2013), in which study the two-dimensional SWE equation using the $\boldsymbol{P_1^{NC} - P_1}$ finite element. We examine that a discontinuous one-dimensional basis function P_1^{NC} does not yet exist, although its two-dimensional version of non-conformal $\boldsymbol{P_1^{NC}}$ basis is well-established (Cui, 2013). In their study, the SWE are approximated in spatially staggered finite element pair due to the use of alternating basis function; conformal basis $\boldsymbol{P_1}$, for free surface variable and a non-conformal $\boldsymbol{P_1^{NC}}$ for horizontal velocity. The terms conformal and non-conformal is related to continuity and discontinuity of the basis function properties. The non-conforming $\boldsymbol{P_1^{NC}}$ shape functions have a value of 1 at one edge, linearly change to -1 to the opposite node, the value at the mid of other two edges are zero. Meanwhile, the $\boldsymbol{P_1}$ shape function have the following properties: it has a value of 0 for all

neighbouring nodes but have a value of 1 at one node (Cui, 2013; Hua & Thomasset, 1984). Unlike the common approach by Hua & Tommaset (1984) and Cui (2013), in this paper, we extend our preceding contribution (Swastika et al., 2020), together with the use of conformal and nonconformal FEM or simply $\boldsymbol{P_1^{NC} - P_1}$ finite element pair to solve 2D SWE in primitive form. Thus, we have derived the novel variational problem based on 2D SWE in primitive form or reformulated again the weak form as well as the discrete formulation. Here we also implement the various boundary condition; absorbing, influx, hardwall and combination thereof to investigate the flexibility of our proposed approach.

The rest of the paper is organized as follows. In Section 2, the governing equation as well as the weak form and the discrete form are examined. In this section, we reformulate the weak formulation using the primitive form of SWE using various boundary conditions. The discrete form is derived by approximating the free surface with a conformal basis $\boldsymbol{P_1}$, but the velocity potential with a non-conformal basis $\boldsymbol{P_1^{NC}}$. In Section 3, we conducted numerical experiment to investigate our proposed formulation using various boundary conditions. We are concerned with the performance of our numerical scheme. The final portion will include conclusions and remarks.

2. Governing Equations and Finite Element Discretization

We begin by discussing the mathematical model used in this paper. Suppose we consider 3D- spatial coordinate system $(\boldsymbol{x}, z)$ where $\boldsymbol{x} = (x, y)$ denoted horizontal coordinate and z represent vertical coordinate. Our discussion focuses on a layer of ideal fluid bounded below by an impermeable bottom topography $z = b(\boldsymbol{x})$ and bounded above by free surface $z = \eta(\boldsymbol{x}, t)$. The total depth denoted by $h(\boldsymbol{x}, t) = d(\boldsymbol{x}) + \eta(\boldsymbol{x}, t)$ where $u(\boldsymbol{x}, t)$ represented horizontal velocity. In this study, we assume that the flow is hydrostatic so the horizontal velocity component is dominant in comparison with the vertical component. Under the assumption that the depth scale is smaller than the horizontal length scale, the fluid motion in the shallow areas is governed by 2D Shallow Water Equations (SWE) in primitive form as follows

$$\frac{\partial \eta}{\partial t} + \nabla.(h\nabla\phi) = 0, \tag{1}$$

$$\frac{\partial \phi}{\partial t} + g\eta = 0, \tag{2}$$

where $g = 9.8 m/s^2$ is the gravitational acceleration. Equations (1) and (2) derived from linearized SWE with irrotational assumptions. In our previous work, we have proposed a one-dimensional finite element scheme to solve the linear SWE (1)-(2) together with the

hard wall boundary conditions. Here we extend our proposed scheme in two-dimensional case with influxing boundaries as well as absorbing boundaries.

To obtain numerical discretization in finite element sense, we start deriving the variational problem of the equations (1) and (2). Suppose Ω be the spatial domain with boundary T and $\boldsymbol{n}$ be the outward unit normal vector. Let ϕ be approximate in a suitable functional space P with the following relation $\nabla\phi.\boldsymbol{n} = 0$ on the boundary T, $\forall\phi \in$ P. Let η also be approximate in a functional space E. The weak form of (1) and (2) is obtained by integrating against a set of admissible test function $V \in E$ and $W \in P$ such that

$$\frac{d}{dt}\int_{\Omega}\eta V d\Omega + \int_{\Omega}\nabla.(d_0\nabla\phi)\,V d\Omega = 0\ ,\forall V \in E, \tag{3}$$

$$\frac{d}{dt}\int_{\Omega}\phi W d\Omega + g\int_{\Omega}\eta W d\Omega = 0\,,\forall W \in P \tag{4}$$

for flat topography $d(\boldsymbol{x}) = d_0$. The second term on equation (3) is integrated by parts using Gauss Theorem to remove velocity potential second derivatives and thus avoid in the contribution of boundary condition

$$\int_{\Omega}\nabla.(d_0\nabla\phi)\,V d\Omega = -\left[d_0\int_{\mathrm{T}}\nabla\phi\,V d\mathrm{T} - d_0\int_{\Omega}\nabla\phi\nabla V d\Omega\right],\forall V \in E, \tag{5}$$

The first term on the right-hand side of (5) vanishes due to hard-wall boundary condition since $\nabla\phi \in P$ and so $\nabla\phi.\boldsymbol{n} = 0$. We obtained the weak form of the equations (1) and (2) as: determine $\eta \in E$ and $\phi \in P$ such that

$$\frac{d}{dt}\int_{\Omega}\eta V d\Omega - d_0\int_{\Omega}\nabla\phi\nabla V d\Omega = 0\ ,\forall V \in E, \tag{6}$$

$$\frac{d}{dt}\int_{\Omega}\phi W d\Omega + g\int_{\Omega}\eta W d\Omega = 0\,,\forall W \in P \tag{7}$$

Furthermore, if we consider the radiation boundary condition (absorbing) given as

$$\phi_t = \pm c\nabla\phi.\boldsymbol{n} \tag{8}$$

then the weak form (6) and (7) must be reformulated. If we consider (5) and employing (8) together with relation (2), we obtained

$$\int_{\Omega}\nabla.(d_0\nabla\phi)\,V d\Omega = \mp c\int_{\mathrm{T}}\eta V d\mathrm{T} + d_0\int_{\Omega}\nabla\phi\nabla V d\Omega\,,\forall V \in E, \tag{9}$$

Thus, the weak form of (1) and (2) with absorbing boundary conditions are given as: determine $\eta \in E$ and $\phi \in P$ such that

Jurnal Matematika Vol. 14, No.1, Juni 2024, pp. 11-21 ISSN: 1693-1394
Article DOI: 10.24843/JMAT.2024.v14.i01.p168

$$\frac{d}{dt}\int_{\Omega}\eta V d\Omega - d_0\int_{\Omega}\nabla\phi\nabla V d\Omega = \mp c\int_{T}\eta V d\mathrm{T}, \qquad \forall V \in E, \tag{10}$$

$$\frac{d}{dt}\int_{\Omega}\phi W d\Omega + g\int_{\Omega}\eta W d\Omega = 0, \qquad \forall W \in P \tag{11}$$

To derive the discrete scheme, we use Galerkin procedure to approximate the weak form as: seek (η^h, ϕ^h) in finite dimensional subspace (E^h, P^h) of finite dimensional space (E, P). We start by writing (η^h, ϕ^h) as linear combination such that

$$\eta^h(\boldsymbol{x}, t) \cong \sum_{j=1}^{N_V}\eta_j(t)T_j(\boldsymbol{x}), \qquad \phi^h(\boldsymbol{x}, t) \cong \sum_{j=1}^{N_S}\phi_j(t)\psi_j(x), \tag{12}$$

where η_j, ψ_j denoted nodal values and N_S, N_V denoted number of segments and vertices of the triangles respectively. Meanwhile, $\{T_j(\boldsymbol{x})\}_{j=0}^{N_V}$ and $\{\psi_j(\boldsymbol{x})\}_{j=0}^{N_S}$ denoted piecewise-polynomial finite element basis functions spanning the approximation spaces E^h and P^h respectively. The $\{T_j(\boldsymbol{x})\}_{j=0}^{N_V}$ is conformal linear basis for shape function P_1 and $\{\psi_j(\boldsymbol{x})\}_{j=0}^{N_S}$ is non-conformal linear basis for shape function P_1^{NC}, see Figure 1 for the illustration. The P_1 shape function have the following properties: it has a value of 0 for all neighbouring nodes but have a value of 1 at one node. Meanwhile, the non-conforming P_1^{NC} shape functions have a value 1 at one edge, linearly change to -1 to the opposite node, the value at the mid of other two edges are zero (Cui, 2013; Hua & Thomasset, 1984).

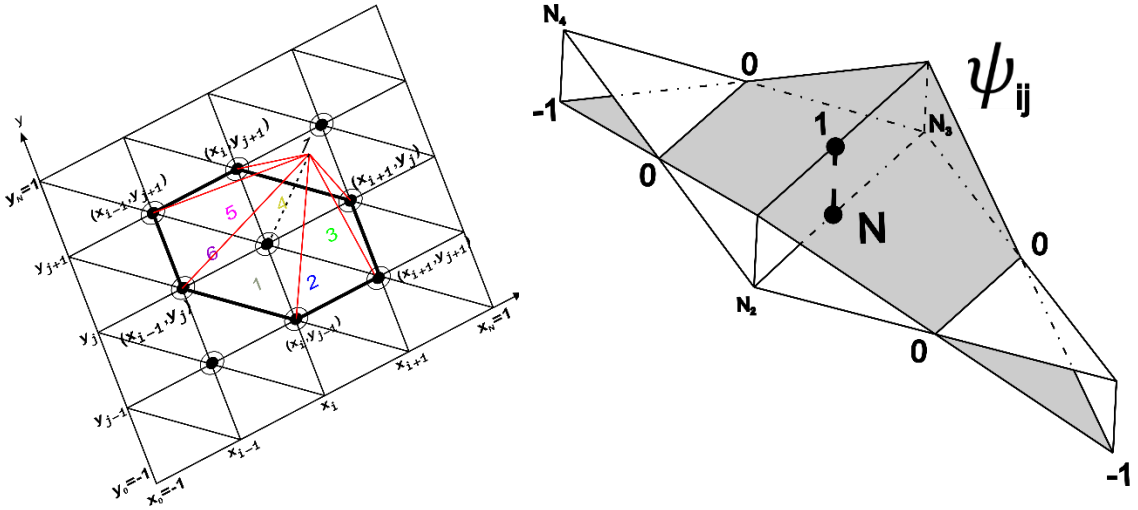

Figure 1. 2D Dimensional shape function; (left) conformal $\boldsymbol{P_1}$ shape function (right), non-conformal $\boldsymbol{P_1^{NC}}$ shape function.

By applying the Galerkin procedure (which orthogonalizes the residual error to the basis functions), the discrete form of Eqs. (10) and (11) can be summarized as: seeking the nodal values η_j, ψ_j such that

$$\frac{d}{dt}\sum_{j=1}^{N_V}\eta_j(t)\int_{\Omega} T_jT_k\,d\Omega - d_0\sum_{j=1}^{\max\{N_V,N_S\}}\phi_j(t)\int_{\Omega}\nabla\psi_j\nabla T_k\,d\Omega = \mp c\sum_{j=1}^{N_V}\eta_j(t)\int_{\partial\Omega} T_jT_k\,d\partial\Omega\,, \tag{13}$$

$$\frac{d}{dt}\sum_{j=1}^{N_V}\phi_j(t)\int_{\Omega}\psi_j\psi_k d\Omega + g\sum_{j=1}^{N_V}\eta_j(t)\int_{\Omega} T_j\psi_k\,d\Omega = 0 \tag{14}$$

The discrete form (13) and (14) can be written in the matrix form as

$$\begin{pmatrix}\boldsymbol{M} & \boldsymbol{0}\\ \boldsymbol{0} & \boldsymbol{M_c}\end{pmatrix}\frac{d}{dt}\boldsymbol{A}(t) = \begin{pmatrix}\boldsymbol{B} & \boldsymbol{S}\\ \bar{\boldsymbol{M}} & \boldsymbol{0}\end{pmatrix}\boldsymbol{A}(t) \tag{15}$$

where the element of mass matrices $\boldsymbol{M}, \bar{\boldsymbol{M}}, \boldsymbol{M_{nc}}$, stiffness $\boldsymbol{S}$ and boundary $\boldsymbol{B}$ formulated as

$$\boldsymbol{A}(t) = [\eta_1, \eta_2, \dots, \eta_N, \phi_1, \phi_2, \dots, \phi_N\,]^T, \qquad \boldsymbol{M} = \left[m_{kj}\right] = \int_{\Omega} T_jT_k\,d\Omega,$$

$$\boldsymbol{M_{nc}} = \left[m^*_{kj}\right] = \int_{\Omega}\psi_j\psi_k\,d\Omega, \qquad \bar{\boldsymbol{M}} = \left[\bar{m}_{kj}\right] = -g\int_{\Omega} T_j\phi_k\,d\Omega,$$

$$\boldsymbol{S} = \left[s_{kj}\right] = \int_{\Omega} d(\boldsymbol{x})\nabla\phi_j\nabla T_k\,d\Omega. \qquad \boldsymbol{B} = \left[b_{kj}\right] = \int_{\partial\Omega} d(\boldsymbol{x})\nabla\phi_j\nabla T_k\,d\partial\Omega,$$

which can be evaluating by any numerical integration method. The term $d(\boldsymbol{x})$ in stifness matrix appears when we consider the varying topography $d(\boldsymbol{x})$. Furthermore, the resulting scheme (15) is an ordinary differential system which can be solved by using any time integration, see (Swastika et al., 2020) for detail reference.

3. Results and Discussion

In this section, the numerical experiments are performed to investigate the implementation of influx boundaries together with absorbing boundaries. For the numerical simulation we take the computational domain as $\boldsymbol{x} \in \Omega_p = [0{,}100] \times [0{,}100], d(\boldsymbol{x}) = d_0 = 10$ which is triangular discretized. Simulation are conducted using steady state at rest or still water level given by

$$\eta(x, y, 0) = 0, \qquad \phi(x, y, 0) = 0,$$

and using absorbing at the three direction, togheter with left influx given by

$$\eta(x = x_l, y = y_l, t) = A\sin(\omega t), \qquad \phi(x = x_l, y = y_l, t) = -\frac{gA}{\omega}\cos(\omega t), \tag{16}$$

with amplitude $A = 1$, angular frequency $\omega = 2\pi f$, $f = 0.1$ and influx zone given as $(x_l, y_l) \in \{(5, y), (x, 5), (25{,}25)\}$. The contour plot of the surface deformation in 3D space along with the top view is presented in Figure 3-6.

From the initial condition of still water level as plotted in Figure 2, the incoming monochromatic wave from the influx zone (x_l, y_l), propagating to the other side with an initial amplitude $A = 1$. In Figure 3 it can be shown that the influx zone is located along the zone $(5, y)$. Due to less finer mesh, the influx zone looks a bit rough. From the left influx boundary condition, a monochromatic function with profile (16) is imposed into the domain and propagates to the upper, lower and right walls. This process is also happening if we impose (16) from right boundary along the zone $(x, 5)$ and propagates to the upper, lower and left walls as shown in Figure 4. Meanwhile, in Figure 5, the influx zone is located along the zone (25,25) and propagates diagonally. Using the absorbing boundary conditions on all four sides together with the influx given by (16) causes a monochromatic wave to propagate and be absorbed on the other side of the wall. Finally, numerical simulation is also conducted using hardwall boundary on four sides of the wall. In Figure 6, the influx zone is located along the zone (25,25) and propagates diagonally towards hardwall boundaries and reflected back to the computational domain. All of these results indicated that our proposed method is flexible in term of using various boundary conditions.

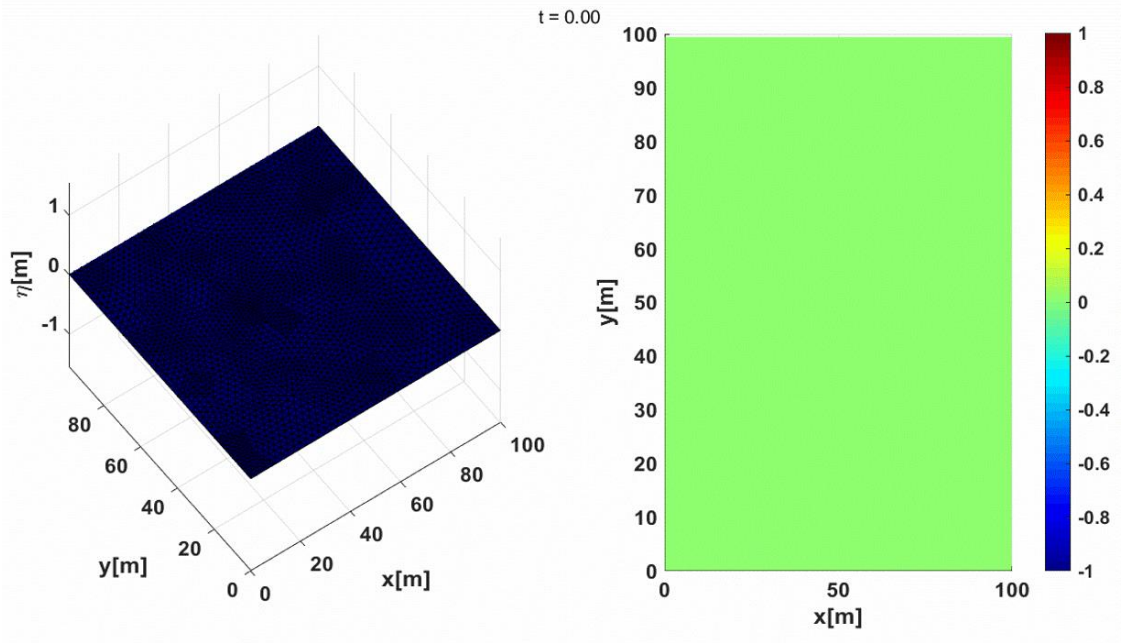

Figure 2. Initial set up; (left) 3D plot of initial condition, (right) top view

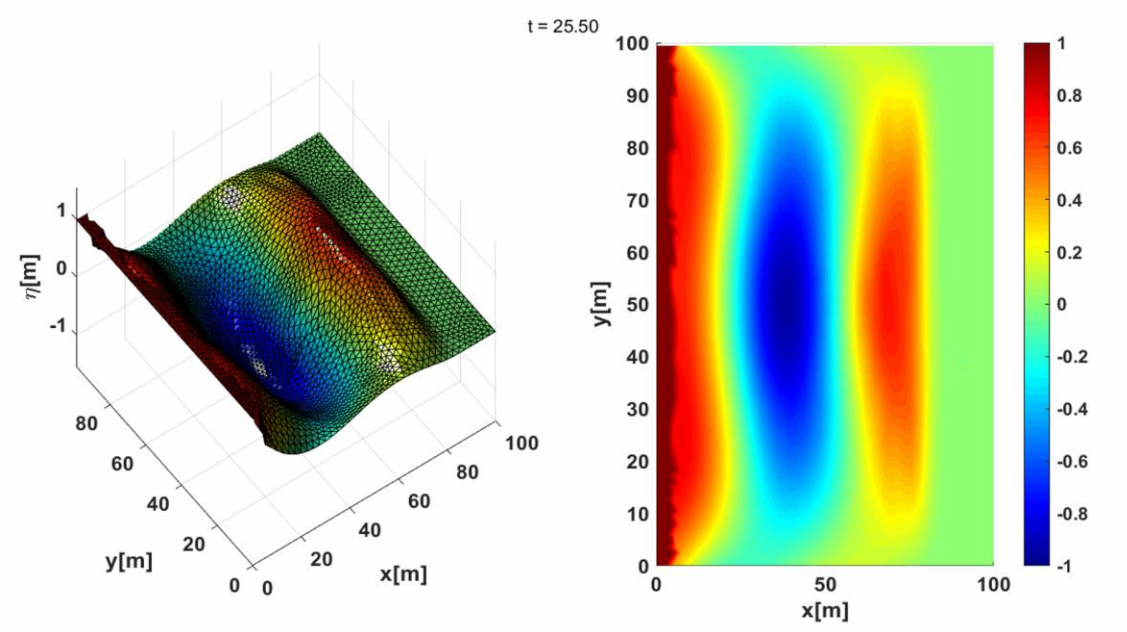

Figure 3. Time-lapse of free surface deformation at the time $t = 25.50$; (left) 3D plot the numerical solution, (right) top view of the problem where it is shown the mono-cromatic influx from $(5, y)$ propagating towards upper, bottom and right boundaries.

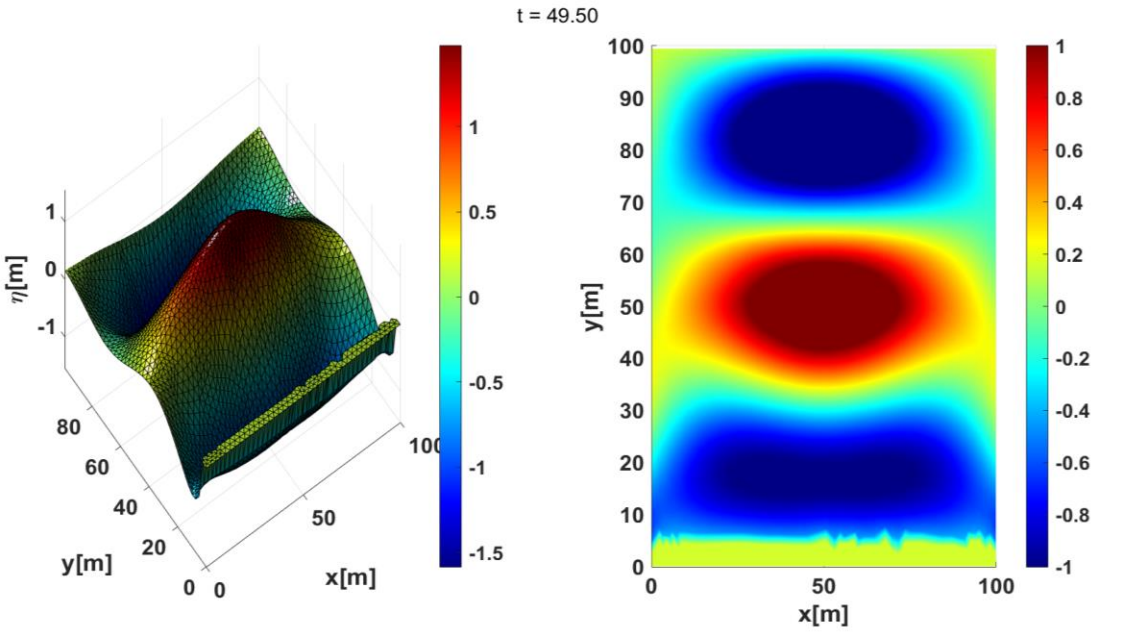

Figure 4. Time-lapse of free surface deformation at the time $t = 49.50$; (left) 3D plot the numerical solution, (right) top view of the problem where it is shown the mono-cromatic influx from $(x, 5)$ propagating towards upper, left and right boundaries.

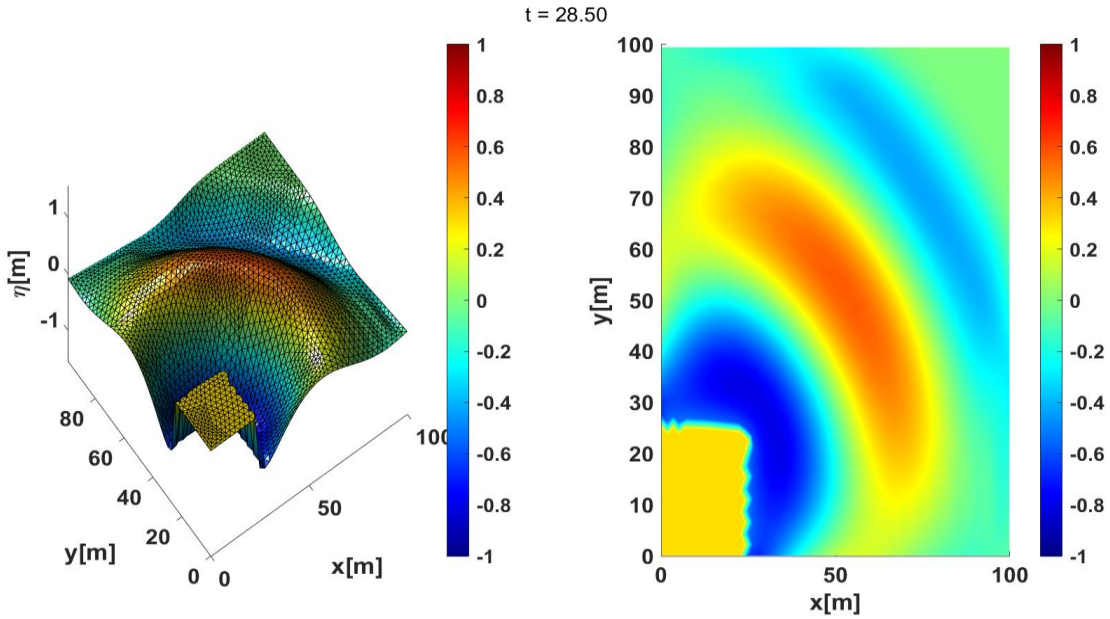

Figure 5. Time-lapse of free surface deformation at the time $t = 28.50$; (left) 3D plot the numerical solution, (right) top view of the problem where it is shown the mono-cromatic influx from $(25,25)$ propagating towards upper, left and right boundaries.

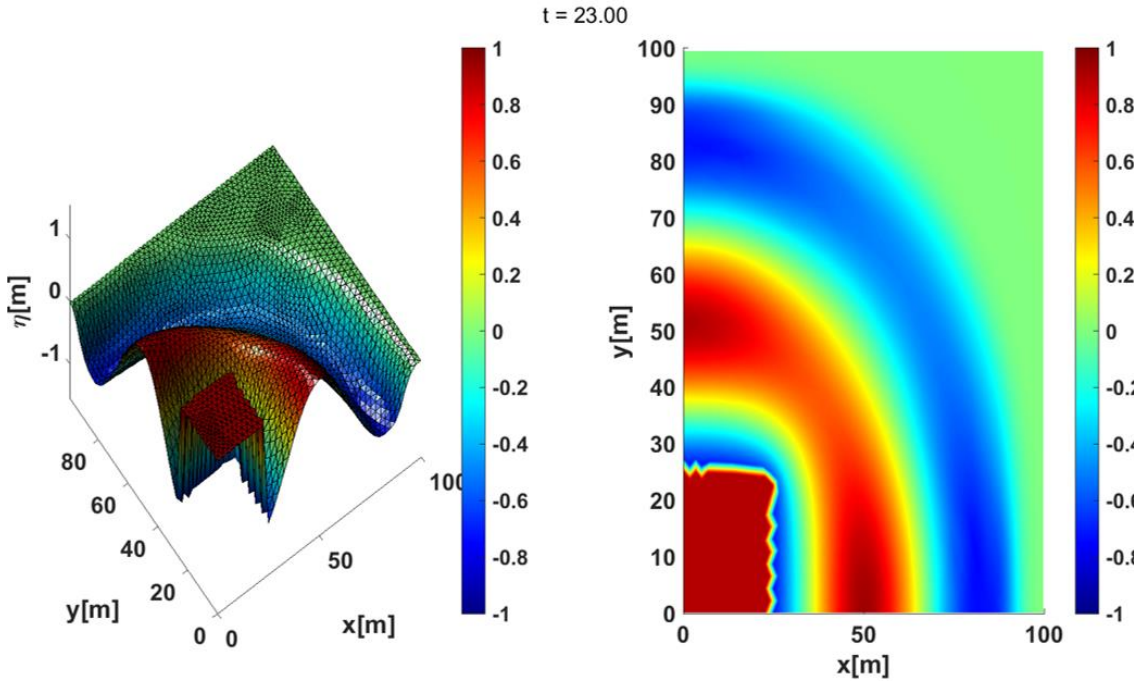

Figure 6. Time-lapse of free surface deformation at the time $t = 23.00$; (left) 3D plot the numerical solution, (right) top view of the problem where it is shown the mono-cromatic influx from $(25,25)$ propagating towards hardwall boundaries.

4. Conclusion and Suggestion

We have presented a novel numerical technique for solving two-dimensional SWE with various boundary conditions. Unlike the common approach suggested by several authors, we have successfully approximated the two-dimensional SWE equation in its primitive form. Here, we approximated the free surface by a linear combination of $\boldsymbol{P_1}$, but the velocity potential is approximated by a linear combination of $\boldsymbol{P_1^{NC}}$. As a result, the variational problem has been successfully reformulated in the primitive form. The use of various boundary conditions, such as an influx, absorbing, hardwall, or a combination thereof, demonstrates the flexibility of our proposed method. Any time-integrated numerical method may readily solve the discrete version, which is a first-order ODE problem. Furthermore, our proposed scheme is explicit, spatially staggered due to the use of an alternating basis function, and easy to implement. Finally, we successfully simulate various cases using several boundary conditions. These studies are relevant for the introduction of our novel finite element method using alternating linear basis conformal and non-conformal to solve 2D SWE in primitive form together with the implementation of various boundary conditions. Our proposed $\boldsymbol{P_1^{NC} - P_1}$ finite element pair will be improved in future research to solve the nonlinear SWE as well as a two-layer case.

References

Cui, H. (2013). *A new numerical model for simulating the propagation of and inundation by tsunami waves* [Delft University of Technology]. https://repository.tudelft.nl/islandora/object/uuid%3Ae82ee739-a03e-441f-bd9e-637c0772ac88?collection=education

Hadiarti, R. N., Pudjaprasetya, S. R., & Swastika, P. V. (2023). The momentum-conserving simulation for shallow water flows in channels with arbitrary cross-sections. *European Journal of Mechanics - B/Fluids*, *99*, 74–83. https://doi.org/10.1016/j.euromechflu.2023.01.001

Hanert, E., Legat, V., & Deleersnijder, E. (2003). A comparison of three finite elements to solve the linear shallow water equations. *Ocean Modelling*, *5*(1), 17–35. https://doi.org/10.1016/S1463-5003(02)00012-4

Hua, B.-L., & Thomasset, F. (1984). A noise-free finite element scheme for the two-layer shallow water equations. *Tellus A*, *36 A*(2), 157–165. https://doi.org/10.1111/j.1600-0870.1984.tb00235.x

Le Roux, D. Y., Sène, A., Rostand, V., & Hanert, E. (2005). On some spurious mode issues in shallow-water models using a linear algebra approach. *Ocean Modelling*, *10*(1-2 SPEC. ISS.), 83–94. https://doi.org/10.1016/j.ocemod.2004.07.008

Siddiqi, A. H. (2018). *Functional Analysis and Applications*. Springer Nature Singapore.

Swastika, P. V., & Pudjaprasetya, S. R. (2021). The Momentum Conserving Scheme for Two-Layer Shallow Flows. *Fluids*, *6*, 346. https://doi.org/10.3390/fluids6100346

Swastika, P. V., Pudjaprasetya, S. R., & Adytia, D. (2020). The P 1 − P NC Finite Element Method for 1D wave simulation using Shallow Water Equations. *IOP Conference Series: Earth and Environmental Science*. https://doi.org/10.1088/1755-1315/618/1/012008

Swastika, P. V., Pudjaprasetya, S. R., Wiryanto, L. H., & Hadiarti, R. N. (2021). A momentum-conserving scheme for flow simulation in 1D channel with obstacle and contraction. *Fluids*, *6*(1), 26. https://doi.org/10.3390/fluids6010026

Tarwidi, D., Pudjaprasetya, S. R., & Adytia, D. (2022). A reduced two-layer non-hydrostatic model for submarine landslide-generated tsunamis. *Applied Ocean Research*, *127*(February), 103306. https://doi.org/10.1016/j.apor.2022.103306